The influence of stabilizers on the performance of Au/TiO_2 catalysts for CO Oxidation

Nating Yang,[1,2] *Samuel Pattisson,*[1] *Mark Douthwaite,*[1] *Gaofeng Zeng,*[2] *Hao Zhang,*[3] *Jingyuan Ma,*[4] *Graham J. Hutchings*[*1]

[1] Max Planck- Cardiff Centre on the Fundamentals of Heterogeneous Catalysis FUNCAT, Cardiff Catalysis Institute, School of Chemistry, Cardiff University, Main Building, Park Place, Cardiff, CF10 3AT, UK

[2] CAS Key Laboratory of Low-Carbon Conversion Science and Engineering, Shanghai Advanced Research Institute (SARI), Chinese Academy of Sciences (CAS), Shanghai 201210, China.

[3] Institute of Functional Nano and Soft Materials Laboratory (FUNSOM), Jiangsu Key Laboratory for Carbon-Based Functional Materials & Devices, Soochow University, Suzhou 215123, China

[4] Shanghai Synchrotron Radiation Facility, Shanghai Advanced Research Institute, Chinese Academy of Sciences, Shanghai 201210, China

*Email. Hutch@cardiff.ac.uk

Keywords： sol-immobilization, stabilizer, Gold, CO oxidation, low coordinated site, monomer, polymer

Abstract

Stabilizers are commonly employed to synthesize nanocrystals with well-defined morphologies and size distributions, making them ideal tools to study structure-activity relationships in heterogeneous catalysts. Whilst it is well documented that stabilizers can influence both the structure and size of the nanocrystals; little emphasis has been placed on how the properties of these species influence catalytic performance. Herein, different polymers (poly-sodium acrylate (PVNaA), poly-vinyl alcohol (PVA) and -vinylpyrrolidone (PVP)) and the monomer sodium acrylate (NaA) were used as stabilizers for the synthesis of Au nanoparticles, supported on TiO_2. The mean Au particle size in all the catalysts were comparable regardless of the stabilizer used, however, the activity of these catalysts towards CO oxidation differed markedly. The activity decreased in the following sequence: Au/TiO_2 (NaA)> Au/TiO_2 (PNaA)> Au/TiO_2 (none)> Au/TiO_2 (PVA)> Au/TiO_2 (PVP), despite the Au/TiO_2 (none) catalyst possessing a larger Au mean particle size, suggesting that active site blocking due to the steric nature of the polymer species. According to UV-vis, XPS, in situ DRIFTS, HRTEM, XAS and composition analysis experiments, it was concluded that the enhanced activity of Au/TiO_2 (NaA) and Au/TiO_2 (PNaA) catalysts were attributed to the large proportions of low coordinate step/kink Au sites. It is to be noted that the electronic interactions between NaA and $HAuCl_4$ facilitated the production of active Au nanoparticles. Our findings highlight that the physicochemical properties of stabilizer can profoundly influence the reactivity of supported metal catalysts prepared by sol-immobilisation. These observations highlight the influence that various stabilizers have on the morphology of supported metal nanoparticles and provides an explanation for the low activity of catalysts prepared using common forms such as PVA and PVP.

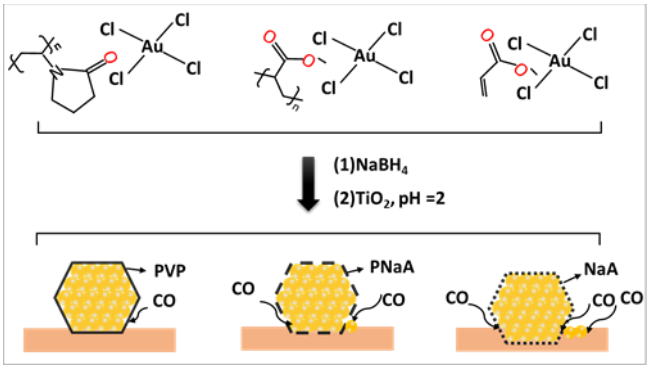

TOC image

Introduction

The influence of particle size on catalyst reactivity is one of the most researched topics in oxidation catalysis.[1-4] Since the seminal work by Haruta and Hutchings in 1980s,[5-7] Au has been reported to be catalytically active for many reactions, including: CO oxidation, acetylene hydrochlorination, epoxidation, hydrogen peroxide synthesis, selective oxidation of hydrocarbons and alcohols, and many other organic reactions.[8-12] For this reason, gold catalysis has been at the forefront of research in this field for many years and consequently. The undercoordinated gold atoms in the perimeter and oxide support are thought to contribute to the catalytic activity of CO oxidation. [13-15] The Au coordination number play key influence on the adsorption of both CO and O_2 from theoretical calculation.[16] Au sites with lower coordination provide stronger bonding for O_2 and CO. H_2O has also been found to play a critical role in the CO oxidation mechanism over Au/TiO_2 catalysts.[17] This has been linked to weakly adsorbed H_2O at the gold-titania interface accepting a proton transfer from the decomposition of *COOH, which was suggested to be rate determining.[18] Numerous methods have been developed to prepare gold catalysts.[19-22] Despite this, many of the methods fail to control the dispersion of Au and as a consequence, the final catalysts often possess wide Au particle size distributions and poorly defined morphologies.[21-22] One technique however, sol-immobilization, employs the use of stabilizers such as polymers, surfactants and polar molecules, which are highly effective at controlling the morphology and particle size distribution.[23] Previously, it was proposed that stabilizers can partially or completely block access of the reactant molecules to catalytic active sites, resulting in a reduction in the perceived catalytic activity.[24-25] Initially, stabilizers are removed by thermal decomposition, for example, PVA in Au/TiO_2 catalysts can be removed by calcination in excess of 300 °C, which lead to dramatic sintering of the supported gold nanoparticles and decrease in CO oxidation.[24] Several advanced methods, including mild or rapid thermal decomposition,[26-27] chemical washing,[24, 28] and UV-ozone treatment,[25, 29] have therefore been further developed to remove stabilizers prior to their application as catalyst. Whilst many such strategies have been developed, explicitly confirming that all the stabilizer is removed is challenging, due to the extremely low quantity of it used in the preparation of these materials. It is therefore pertinent to assess how these stabilizers influence catalytic performance, both sterically and electronically.[30]

In homogeneous Au catalysis, ligands are employed to provide steric and electronic influence to control reaction selectivity.[31] Interestingly, some studies report that stabilizing ligands can also influence the performance of metal nanocrystals in hetero-catalytic applications, particularly with regard to reaction selectivity.[20, 23, 32] For example, the presence of PVA in Au/TiO_2 catalysts has been reported to increase the stability of the supported Au nanoparticles, upon recycling. The residual PVA was also found to enhance the activity of the Au/TiO_2 for the oxidation of glycerol.[20] Similarly, residual PVP present in a Au/SiO_2 was determined to significantly improve activity towards p-chloronitrobenzene hydrogenation.[25] Moreover, Au clusters stabilized by PVP with size smaller than 1.5 nm showed higher activity for aerobic oxidation of alcohol than those of larger Au clusters that stabilized by poly(allylamine). It was proposed by the authors that the Au clusters are negatively charged by electron donation from PVP and have higher electron density on the Au core, which leads to the improvement in catalytic activity.[33]

Despite the abundance of studies which employ the use of stabilizers in catalyst synthesis, investigations into whether they promote catalysis are surprisingly scarce. If stabilizers can promote catalysis, they should be considered in catalyst design. After all, local chemical environments are incredibly important for directing catalysis in both homogeneous catalysis and bio catalysis. We therefore set out to prepare a series of catalysts with a range of stabilizers, which have different electron interaction with $HAuCl_4$ probed by UV-vis spectroscopy. Then the simple, well established, reaction (CO oxidation) was used as a model to investigated how those stabilizers influenced the catalytic performance of Au/TiO_2 catalysts. Through combining extensive characterization and testing, mono- and polymeric sodium acrylate (NaA and PNaA) were found to have a positive effect on catalyst performance for the oxidation of CO. The beneficial effect of the mono- and polymeric sodium acrylate stabilizer was further probed by in-situ Diffuse Reflectance Infrared Fourier Transform Spectroscopy (in situ DRIFTS), HRTEM, and XAS, which demonstrated that activity of the catalysts correlated with proportions of low co-ordinate step/kink Au sites.

Experimental section

Chemicals (Source, Purity)

Carbon Monoxide (5000 ppm in synthetic air) was purchased from BOC, $HAuCl_4 \cdot xH_2O$ (99.8 %) was purchased from Strem. $NaBH_4$ (powder,≥98%), Polyvinylpyrrolidone (PVP, M_w =10000), polyvinyl alcohol (PVA, 80% hydrolysed M_w=9000-10000), sodium acrylate (NaA, 97%), and sodium polyacrylate (PNaA, M_w=8000, 45 wt.% in H_2O) were purchased from Sigma Aldrich. TiO_2 (P25) was purchased from Evonik. All chemicals were used as received.

Catalyst Synthesis

All the catalysts have been prepared in line with a procedure documented in the literature;[34] only slight modifications have been incorporated. For a typical synthesis of a 2.0 g of 1 wt.% Au/TiO_2 catalyst used in this study, aqueous solutions of $HAuCl_4$ (1.6 mL, 0.062 M) and stabilizer (2 mL, 0.059 M in terms of the monomeric unit) were first combined in a vial and stirred for 15 mins. The mixture was subsequently added to a beaker and diluted to a stated quantity, either 300 or 800 mL, followed by vigorous stirring. Following this, fresh aqueous $NaBH_4$ (2 mL, 0.127 M) was added rapidly, forming a dark red sol indicative of the formation of small reduced Au nanoparticles.[35-36] After a further 30 mins of stirring, the Au nanoparticles were immobilized onto the support by the instantaneous addition of TiO_2 (1.98 g) and dropwise acidification of the solution to pH = 2 with sulfuric acid, during which the support surface with positive charges strongly interacts with the negatively charged gold particles.[20,37-38] The reaction mixture was then left to stir for an additional 1 hour before being filtered under vacuum and washed with 40 mL of deionized water 5 times (200 mL in total). Finally, the catalyst was recovered and dried at (110 ^oC, 16 h) before being crushed into a fine powder using an agate mortar and pestle.

The preparative procedure, outlined above, was used for the preparation of various 1wt.% Au/TiO_2 catalysts using different stabilizers. The stabilizers used were sodium acrylate, polymeric sodium acrylate, polyvinyl alcohol (PVA) and polyvinyl pyrrolidone (PVP). This procedure was also used to prepare an analogous 'stabilizer-free' catalyst; for this, no stabilizer was added to the aqueous $HAuCl_4$ at the beginning of the procedure.

Catalyst evaluation for CO oxidation

The activity of each of the catalysts was assessed for CO oxidation, which was carried out in a fixed bed reactor and performance quantified using an online micro-GC. Each test was carried out by loading catalyst (50 mg) into U-shaped glass reactor tube (3-mm internal diameter), which was plugged using two aliquots of quartz wool. The reactor bed was subsequently immersed in a thermostatic water bath (60 °C). A flow of CO in air (20 mL·min^{-1}, 5000 ppm) was then introduced into the reactor, corresponding to a GHSV of 24,000 mL·g^{-1}·h^{-1}. The micro-GC was equipped with a 1.5 m packed carbo-sieve column and possessed an automated injection valve and a thermo conductivity detector (TCD).

Au dispersion was estimated from the following equation by assuming the spherical particles, [39] where the mean diameter is obtained from STEM results.

$$\text{Au dispersion} = \frac{1.12}{\text{Au diameter (nm)}}$$

Activity was assessed by the following equation.

$$\text{Activity} = \frac{\text{mol}_{\text{CO converted}}}{\text{mol}_{\text{Au}} \cdot \text{h}}$$

CO conversion and activity associated errors were calculated from standard deviation of at least 3 different batches of catalysts.

Diffuse reflectance infrared fourier transform spectroscopy (DRIFTS) experiments were conducted using a Bruker Tensor 27 spectrometer with a Praying Mantis high temperature (HVC-DRP-4) cell chamber. For these experiments, first a background spectrum was obtained by flowing 2% CO, 8% Ar, and 90% N_2 over KBr. The catalyst was subsequently placed into the cell and a flow of nitrogen (30 ml·min^{-1}) was passed over it, to remove any residual air. Finally, a flow of 2% CO, 8% Ar, and 90% N_2 was passed over the catalyst and a spectrum was recorded every 20 seconds until stabilization of gas and spectrum was achieved.

Powder X-ray diffraction (XRD) patterns were collected on a PANalytical MPD diffractometer fitted with a Cu Kα radiation source at ambient conditions. Samples were scanned in the range of 20-80 ° at 40 kV and 40 mA.

XPS was performed on a Kratos Axis Ultra-DLD photoelectron spectrometer, using monochromatic Al Kα radiation (hν = 1486.6 eV) at 72 W (6 mA×12 kV) power. High resolution and survey scans were performed at pass energies of 40 and 150 eV respectively. The

data were analyzed by Avantage software of Thermo. Correction of the charge effect was made with the C1s peak at 284.8 eV.

The loading of sodium acrylate on the catalyst was estimated through consideration of the feed amount of NaA minus the amount of NaA that remaining in solution after the synthesis solution. For this, the concentration of NaA remaining was quantified by high-performance liquid chromatography (HPLC), equipped with refractive index and diode array detectors. A Metacarb 67H column was used to separate the products at 50 ºC with an isocratic mobile phase of H_3PO_4 (0.1 % in H_2O) and a flow rate of 0.8 mL/min.

The loading of gold, sodium and boron on each of the catalysts was quantified by microwave plasma atomic emission spectroscopy (Agilent 4100 MP-AES). Catalyst (~10 mg) was digested in freshly prepared aqua regia (5 mL). The solution was diluted to a total of 50 mL and filtered in preparation for analysis. Elemental concentrations were then quantified against analytical standards.

Scanning Electron Microscopy was performed using a Tescan Maia3 field emission gun scanning electron microscope (FEG-SEM) operating at 30 kV. Images were acquired using the secondary electron and backscattered electron detectors. Bright field scanning transmission electron images (STEM) were obtained using a STEM holder. Samples were dispersed as a powder onto 300 mesh copper grids coated with Holey carbon film.

High-resolution transmission electron micrographs (HR-TEM) were acquired using JEOL JEM-ARM200F transmission electron microscope equipped with energy dispersive X-ray spectroscopy (EDS) at 200 kV.

The measurements of X-ray absorption near-edge structure (XANES) and extended X-ray absorption fine structure (EXAFS) of Au L3-edge were carried out on the XAFS station of BL14W1 beam-line of Shanghai Synchrotron Radiation Facility. Utilizing the ATHENA module embedded in IFEFFIT software packages, all XAFS data were performed following the standard procedures. The EXAFS contributions were separated from different coordination shells by using a hanning windows (dk=1.0 $Å^{-1}$). Subsequently, the quantitative curve-fittings were carried out in the R-space (1.5-3.4 Å) with a Fourier transform k-space range of 3.30-10.0 $Å^{-1}$ by using the module ARTEMIS of IFEFFIT.

UV-Vis spectra were collected with a HP8453 spectrophotometer using a quartz 1-cm

pathlength cell. The aqueous solutions of $HAuCl_4$ (0.062 M), stabilizer (0.059 M), and the mixture of $HAuCl_4$ and the stabilizer (mixed and stirred in a vial for 15 min) were diluted and tested under room temperature.

Results and discussion

For the preparation of Au/TiO_2 catalysts, new stabilizers (NaA and PNaA) and traditional stabilizers (PVP and PVA) were chosen as the protecting ligand for Au during the sol-immobilisation synthesis. Initially, the interaction between the different stabilizers and $AuCl_4^-$ were studied with UV-vis spectra. The aqueous solutions (aq) of these stabilizers exhibited no adsorption peak at between 200-900 nm (Figure 1(a)). While the chloroauric acid (aq) showed a strong absorption band at 217 nm and a weak one at 290 nm (Figure 1(b)). These bands are indicative of the d-d charge transfer band of Au^{3+} and the chloro-to-Au charge transfer bands of $AuCl_4^-$, [40-42] respectively. Upon the combination of $HAuCl_4$ (aq) and PVP (aq), the original band red-shifts to 214 nm with a shoulder peak at 206 nm, which could be ascribed to the formation strong electronic interaction between Au^{3+} and the hydroxyl end groups of PVP, as the hydroxyl end groups of PVP serve as a very mild reductant.[43] Similarly, the combination of $HAuCl_4$ (aq) and NaA (aq) leads to the red shifting of original band to 205 nm, suggesting that the formation of a stronger electronic interaction between Au^{3+} and sodium acrylate. The results suggest that electronic and geometric interaction between $HAuCl_4$ and NaA are likely responsible for suppressing Au nanoparticle agglomeration, through static exclusion and steric hinderance. In each case of Au/TiO_2 with stabilizer, the quantity of stabilizer used was equimolar, in terms of the monomeric unit. The mean particle size for each of the stablised catalysts was comparable from STEM images (Figure S1), ranging from 3.6 to 4.7 nm in diameter. For comparative purposes, a stabilizer-free 1 wt.% Au/TiO_2 (Au/TiO_2 (none)) catalyst was also prepared and rather unsurprisingly possessed slightly larger Au nanoparticles (5.4 nm). These results highlight the stabilizers influence on particle size. Some particle stabilization can be induced from BH_4^-, $B(OH)_4^-$ and Na^+ species, in the absence of an organic stabilizer,[44] but are evidently less effective.

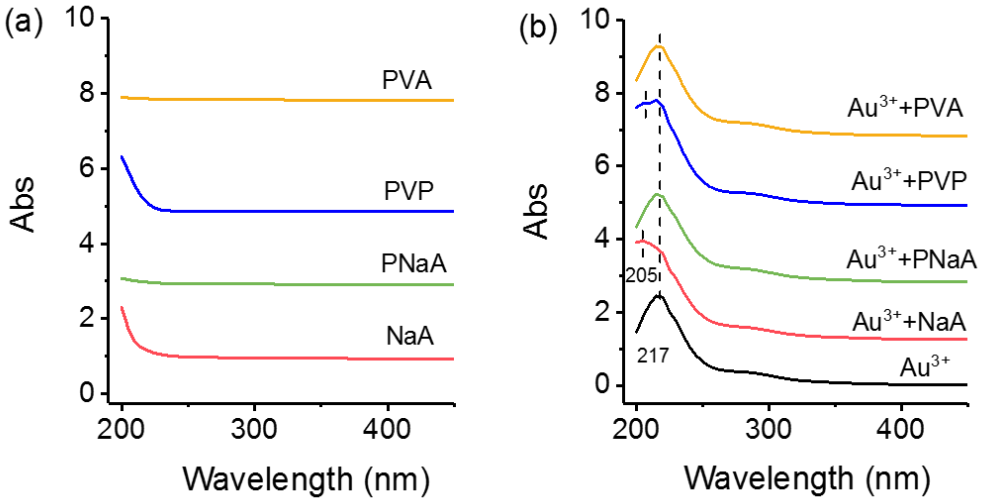

Figure 1. UV-vis spectra of aqueous solution of (a) stabilizers and (b) the mixture of chloroauric acid and stabilizer.

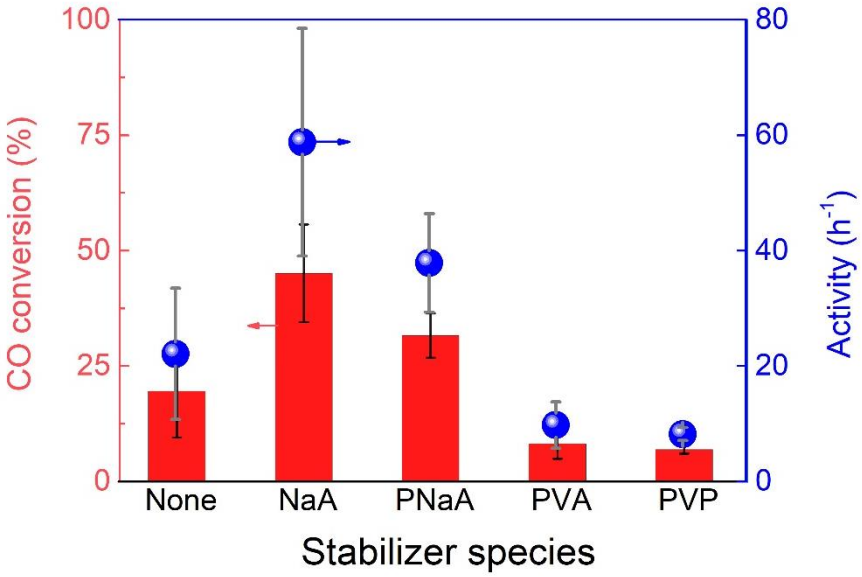

Figure 2. Performance of Au/TiO_2 catalysts in CO oxidation. The influence of the stabilizer ligand is investigated. Catalysts were prepared using a water/catalyst ratio of 0.4 L/g. Reaction conditions: SV=24, 000 $mL \cdot g^{-1} \cdot h^{-1}$, T=60 °C. The activity is calculated based on Au content measured from MP-AES. Associated errors were calculated from standard deviation of at least 3 different batches of catalysts.

To investigate the influence the different stabilizers had on catalytic performance, each of

the synthesized catalysts were subsequently employed for the oxidation of CO. The activity of each catalyst is highlighted in Figure 2 and Table 1. Interestingly, catalytic performance varied quite significantly between different batches of the same catalyst, highlighted by the associated error bars in Figure 2. It is possible that this may have been attributed to different quantities of the stabilizer(s) incorporated into the final catalyst, influencing the resultant Au particle size. Notably, this poor reproducibility was observed with all the catalysts, regardless of the stabilizer employed. The activity of the catalysts examined decreased in the following sequence: Au/TiO_2 (NaA) > Au/TiO_2 (PNaA) > Au/TiO_2 (none) > Au/TiO_2 (PVA) > Au/TiO_2 (PVP). Evidently, the performance is not solely attributed to the size of the supported metal nanoparticles, as the Au/TiO_2 prepared with PVP was the least active, despite possessing the smallest mean particle size (3.6 nm). This is in stark contrast to previous reports,[45] which suggest that catalytic activity of Au supported catalysts in this reaction is entirely dependent on particle size in the range of 3-9 nm. This contradiction is further underlined by the fact that the stabilizer-free catalyst (Au/TiO_2 (none)), which possesses the largest mean particle size and is more active than the analogous catalysts prepared using PVA and PVP (12.8 h^{-1} vs. 12.3 and 8.7 h^{-1}). It is therefore clear, that some additional effects from the stabilizers are contributing to the performance of these catalysts.

Table 1. Loading of Au, B, and Na, average size of Au nanoparticles, and catalytic activity of fresh catalysts prepared under water/catalyst= 0.4 L/g.

Catalysts	Au content [a] (wt.%)	B content [a] (wt.%)	Na content [a] (wt.%)	Au NP average size [b] (nm)	CO conversion (%)	Activity [c] (h^{-1})
Au/TiO_2 (none)	0.88	0.02	0.08	5.4	10.7	12.8
Au/TiO_2 (NaA)	0.87	0.01	0.15	4.3	36.8	44.6
Au/TiO_2 (PNaA)	0.96	0.01	0.18	4.0	31.0	34.1
Au/TiO_2 (PVA)	0.86	0.05	0.24	4.7	10.0	12.3

Au/TiO_2 (PVP)	0.86	0.04	0.21	3.6	7.1	8.7

[a] Measured from MP-AES, [b] Calculated from SEM images (Figure S1), [c] Calculated based on Au content measured from MP-AES.

Further characterization was conducted to determine whether the difference in reactivity between the catalysts was attributed to elemental composition, morphology or electronic properties. All the characterisation conducted is of the same batch, so that any trends in physicochemical properties could be aligned directly to activity. MP-AES results confirmed that the Au loading (Table 1, Column 2) in each of the catalysts varied quite drastically (0.81 – 0.96 wt.% Au). However, after normalizing the activity to Au content and dispersion (Table 1, Column 7) substantial differences in performance remained. Despite previous publications suggesting that Na and BH_4^- components that introduced from synthesis have strong bond with Au cores,[28, 44] in this work, no correlation between the quantity of these components and reactivity was observed. Moreover, through inspection of the Au 4f XPS spectra (Figure S2), the binding energies for the Au $4f_{7/2}$ species in each of the catalysts were ranging from 83.5 to 83.7 eV. This is notably lower than the analogous binding energy observed for metallic Au foil (84.0 eV), which is attributed to the under-coordinated surface atoms on nanoparticles. Such atoms shifts the associated Fermi level to a lower energy, reducing the energy required to eject electrons from the metal.[42] Given that there were no notable differences in the binding energy of the $Au4f_{7/2}$ species, the stabilizers evidently have no influence on electronic properties of the Au nanoparticles. The differences in performance they exhibit for CO oxidation could therefore not be attributed to any observable electronic effect. TG-MS was unable to distinguish the small amounts of ligand present on the catalysts (Figure S3). Approximately 85% of fed NaA remained on the catalyst after synthesis, calculated from using HPLC to quantify the amount of residual stabiliser left in solution after the preparation.

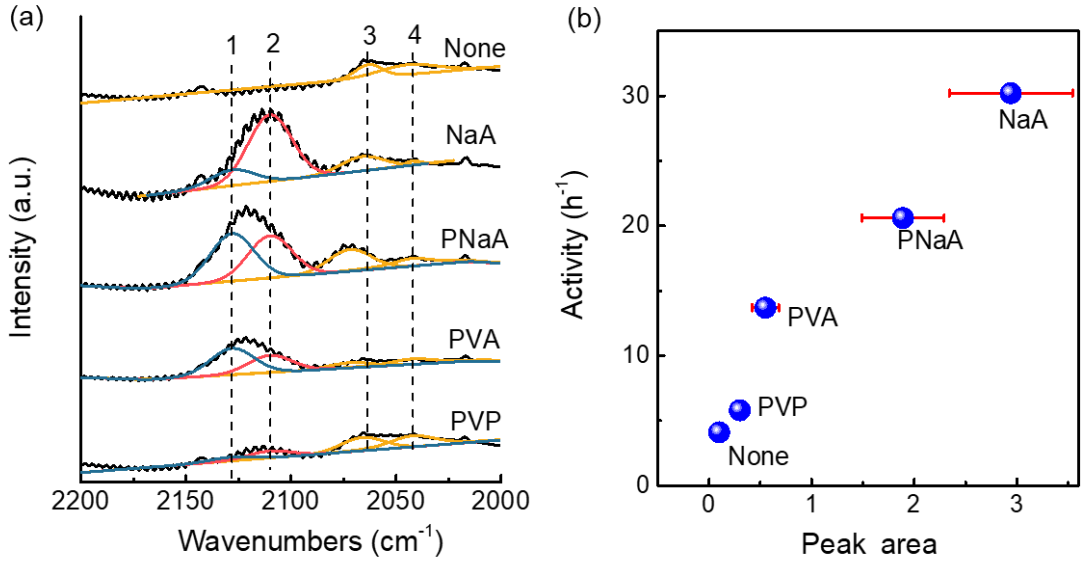

Figure 3. (a) CO diffuse reflectance infrared Fourier transform spectroscopy (CO-DRIFTS) of the catalysts at room temperature. Feed gas: 2% CO, 8% Ar, and 90% N_2. (b) The correlation between the activity and area of peak 2 (2110 cm^{-1}) over different catalysts, the error bars are standard deviation from 3 times of CO-DRIFTS tests. The catalysts were prepared under water/catalyst= 0.4 L/g and stored for 50 days before the tests (Table S1)).

A series of CO-DRIFTS experiments were subsequently conducted on the catalysts after 50 days of storage (Table S1). All catalysts showed deactivation in activity after storage, which is probably due to Au (III) reduction, Au nanoparticle agglomeration, loss of surface hydroxyl groups, loss of surface moisture, and accumulation of surface carbonates and formates.[46] In the associated spectra (Figure 3(a)), two sets of asymmetric bands are observed between 2000-2200 cm^{-1}. The relative intensity of these two bands differed significantly depending on which stabilizer, if any, was used in the preparation of the catalyst. Previously, researchers have correlated the intensity of these two asymmetric bands with reactivity in the oxidation of CO.[34] Given that the adsorption bands were not symmetric in nature, it was possible to deconvolute the adsorption bands further; the two asymmetric bands were separated into four symmetric bands centered at 2128 (Peak 1), 2110 (Peak 2), 2072 (Peak 3) and 2042 (Peak 4) cm^{-1}. Through consultation of previous literature, these could be assigned to CO bound to specific Au sites, such as: metallic or positively polarized gold sites (Peak 1),[47-48] low coordinated step/kink gold sites (Peak 2)[47] and negatively charged gold sites (Peaks 3 and 4).[48] Interestingly, we found a

strong correlation between the area of peak 2, low co-ordinate step/kink sites, and activity towards CO oxidation (Figure 3(b)). This is consistent with previous suggestions that the population of such sites in supported Au catalysts correlate with performance in CO oxidation.[49] In this context, the results presented in Figure 3 indicate that the stabilizer used in the preparative stage can dramatically influence both the structure and morphology of the Au nanoparticles in the final catalyst.

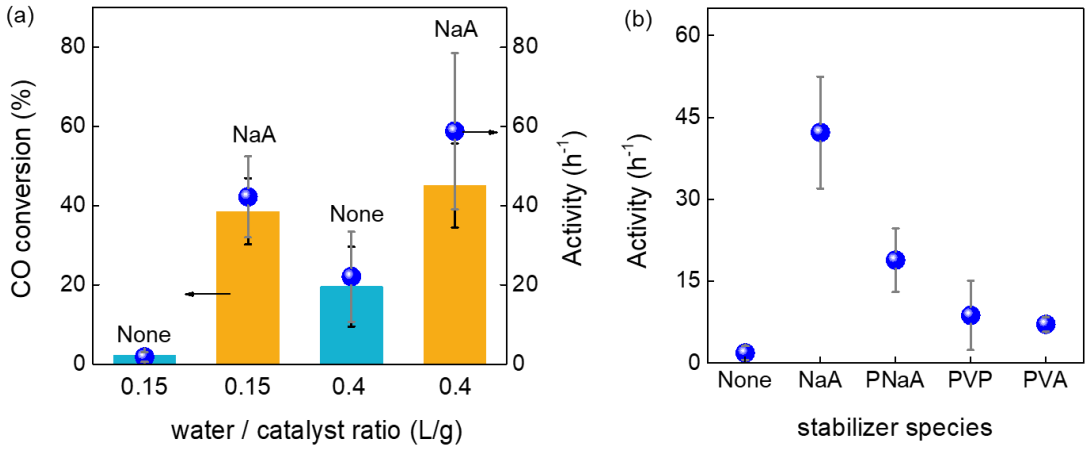

Figure 4. (a) Influence of the ratio of water volume to catalyst weight on the catalytic performance of the stabilizer-free and sodium acrylate stabilized catalyst. (b) Activity of catalysts prepared with different stabilizing ligands towards CO oxidation. Catalysts were prepared using a water/catalyst ratio of 0.15 L/g. Reaction conditions: SV=24, 000 mL·g^{-1}·h^{-1}, T=60 °C. The associated errors were calculated from standard deviation of at least 3 different batches of catalysts.

Table 2. Loading of Au, B and Na, average size of Au nanoparticles, and catalytic activity of fresh catalysts prepared under water/catalyst= 0.15 L/g.

Catalysts	Au Content [a] (wt.%)	B Content [a] (wt.%)	Na Content [a] (wt.%)	Au NP Average size [b] (nm)	CO Conversion (%)	Activity[c] (h^{-1})
Au/TiO$_2$ (none)	0.82	0.02	0.11	11.2	1.7	2.2

Au/TiO_2 (NaA)	0.86	0.01	0.08	4.4	33.7	41.4
Au/TiO_2 (PNaA)	0.89	0.01	0.09	4.4	13.7	16.2
Au/TiO_2 (PVA)	0.80	0.01	0.11	4.1	5.6	5.9
Au/TiO_2 (PVP)	0.90	0.02	0.12	4.9	5.0	7.4

[a] Measured from MP-AES, [b] Calculated from STEM images (Figure S4), [c] Calculated based on Au content measured from MP-AES.

As highlighted in Figure 2, although differences in reactivity appear to be influenced by the stabilizer used in the preparation, a large degree of error in the reactivity was observed when the preparative procedure was repeated. Such error is probably associated with variation in the population of small clusters as these are considered to be the active species.[13, 15] It was therefore important to ensure that the observed trends were consistent and so, the preparation procedure was altered in an attempt to improve reproducibility. Given that stabilizers are often employed to control particle size (and prevent agglomeration), it was hypothesized that the quantity of water used in the preparation could influence both the reproducibility and activity of the catalysts.[50] For this reason, a series of additional sodium acrylate stabilized catalysts were prepared using different quantities of water and were tested for CO oxidation (Figure 4(a)). It was found that the reproducibility is markedly improved when the water/catalyst ratio used in the preparation reduced from 0.4 to 0.15 L/g. In the same time, the activity of the catalysts with NaA slightly decreased (44.6 to 41.4 h^{-1}) while that of Au/TiO_2 (none) markedly decreased (12.8 to 2.2 h^{-1}). Moreover, as shown in Figure 4(b), clear differences in performance could be observed between the catalysts with different stabilizers prepared from less water, and the Au/TiO_2 (NaA) catalyst exhibited the highest activity. It is obvious that Au NPs without stabilizer are more susceptible to aggregation (average size is 11.2 nm) than those with stabilizers (4.1-4.9 nm) when less water was present in the preparation (Figure S4), therefore Au/TiO_2 (none) shows lower activity and error. The influence of any composition discrepancy and any electronic effects on catalyst performance can be excluded (Table 2 and Figure S5). The increased reactivity is also correlated with an increased amount of low coordinated Au sites

(Figure 5). Evidently, NaA and PNaA stabilizers can still promote the formation of more low coordinated step/kink gold sites despite the concentrating of reaction solution.

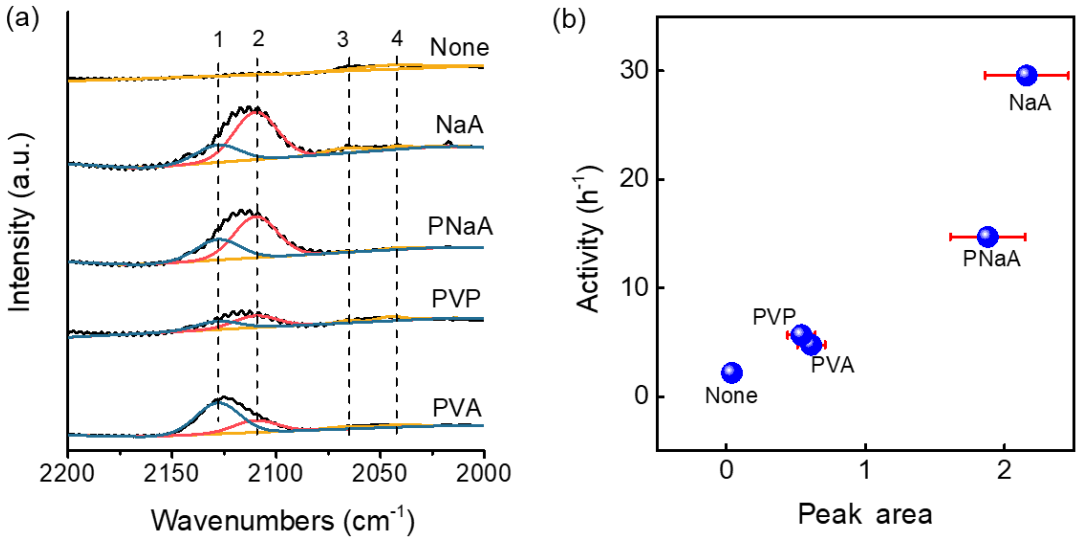

Figure 5. (a) In-situ diffuse reflectance infrared Fourier transform spectroscopy (DRIFTS) of catalysts at room temperature. Feed gas: 2% CO, 8% Ar, and 90% N_2. (b) The correlation between area of peak 2 (2110 cm^{-1}) and the activity over different catalysts. The error bars are standard deviation from 3 times of CO-DRIFTS tests. The catalysts are prepared under water/catalyst= 0.15 L/g and stored for 21 days before the tests (Table S2).

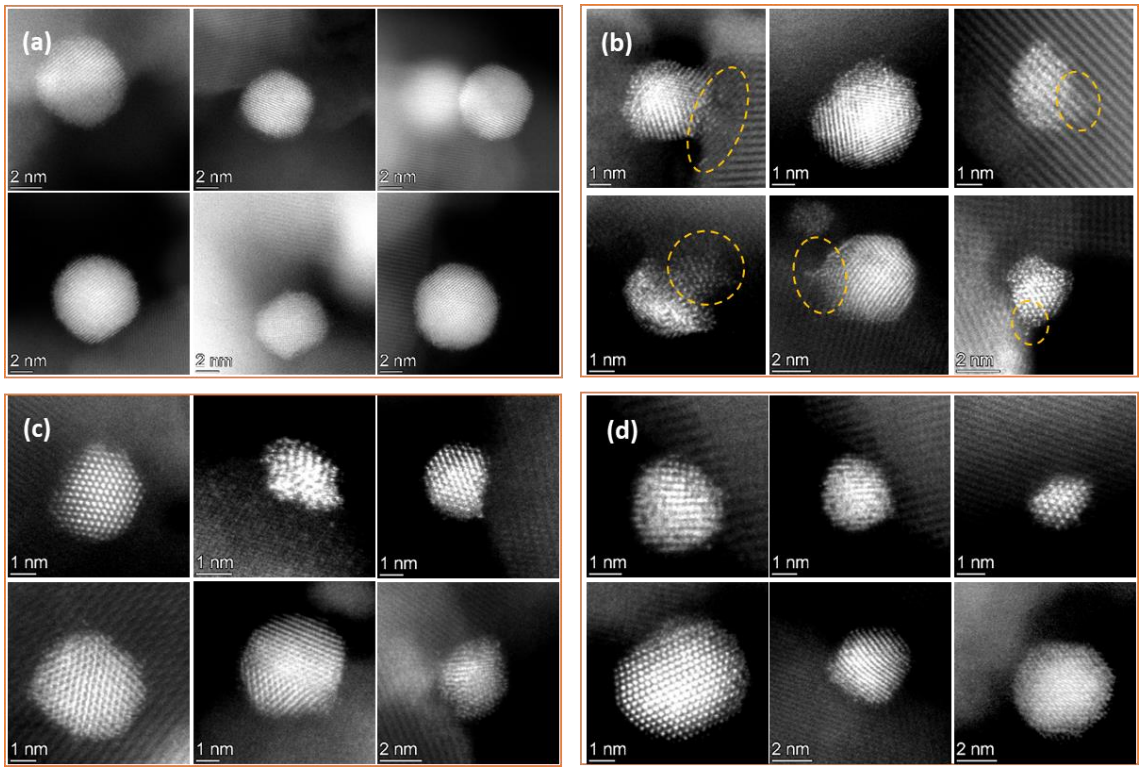

Figure 6. High resolution TEM images of catalyst (prepared under water/catalyst= 0.15 L/g) (a) Au/TiO_2(none), (b) Au/TiO_2(NaA), (c) Au/TiO_2(PNaA), and (d) Au/TiO_2(PVP).

High Resolution Transmission Electron Microscopy (HR-TEM) was conducted on the series of catalysts to further elucidate the influence of each stabilizer. Figure 6(b-c) clearly demonstrates that using NaA, PNaA or PVP as a stabilizer, results in smaller Au particles (2.9 – 3.2 nm). Qualitatively, it can also be observed that these stabilizers facilitate the production of polyhedron-type Au particles, as opposed to larger (7.2 nm) and more spherical Au particles observed in the stabilizer free sample (Figure 6(a) and Figure S7(a-b)). The NaA stabilized sample (Figure 6(b)), which was shown to be the most active catalyst, contains a high proportion of small, flat Au clusters as highlighted. These features appear to be less common in the PNaA stabilized sample (Figure 6(c)), are rarely observed in the highly regular de-wetted PVP stabilized material (Figure 6(d)) and completely absent in the stabilizer free sample (Figure 6(a)). It is well documented that the active site for CO oxidation over Au catalysts supported on reducible oxides is at the metal-support interface.[51] It is therefore unsurprising that the most active catalyst is one which possesses a higher (qualitative assessment) proportion of small, flat Au clusters.

XAS measurements were also conducted to probe the chemical state and coordinative

environment of Au species. As shown in the XANES spectra in Figure 7(a), all the samples (the activities are shown in Figure S8) share similar spectral features with that of Au foil, which indicates the metallic state of Au in these samples prepared by sol immobilisation method. The k^2-weighted Fourier transform of Au L3-edge extended X-ray absorption fine structure (EXAFS) spectra of these samples (Figure 7(b)) exhibited characteristic peak attributable to Au-Au bond. A quantitative curve-fitting analysis revealed that the coordination number (CN) of the Au-Au bonding in the first shell is estimated to be 11.5, 10.9, 9.3, and 10.2 for Au/TiO_2 (none), Au/TiO_2 (NaA), Au/TiO_2 (PNaA), and Au/TiO_2 (PVP) respectively, at a distance of *ca.* 2.83-2.86 Å (dashed line in Figure 7(b) and Table S3). As proposed in Figure 8, these results suggest that the presence of NaA in the synthesis, promotes the formation of lower coordinated Au nanoparticles. When compared with the CO-DRIFT result, the lower peak area for peak 2 in samples with PNaA or PVP (compared to NaA), is likely to be due to the blocking effect of the polymer.

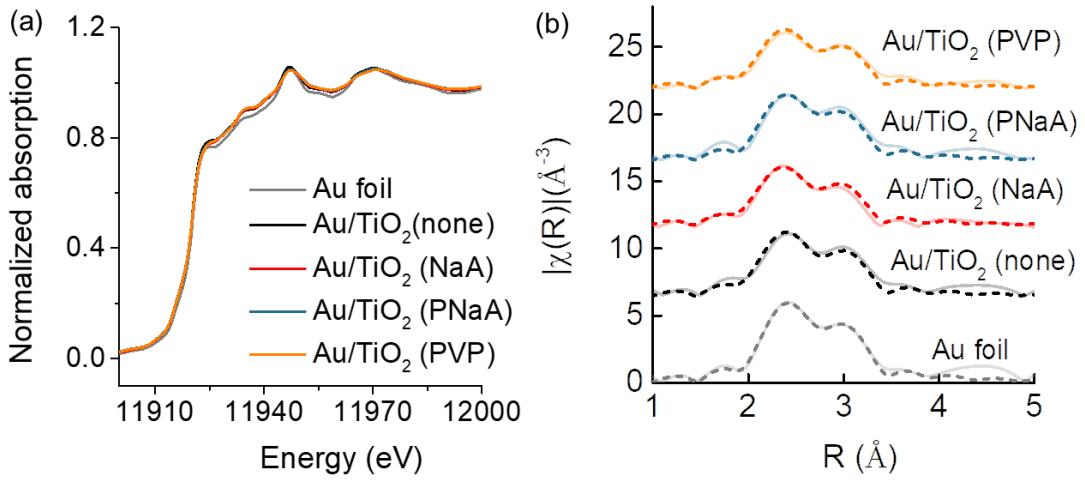

Figure 7. (a) Au L3 edge-normalized XANES spectra of the samples and reference material of Au foil; (b) The k^2-weighted Fourier transform spectra of Au L3-edge EXAFS data for the Au foil and the samples (solid line), and their fitting spectra (dashed line).

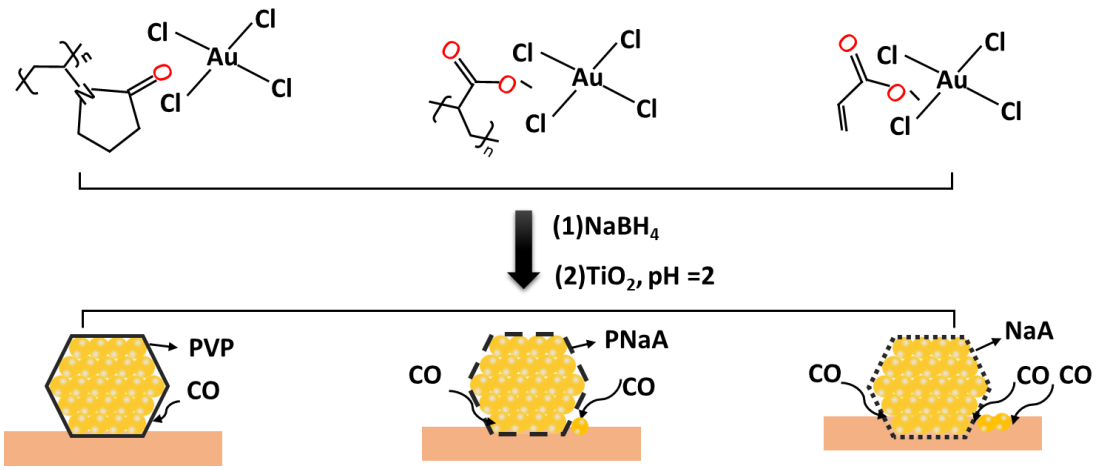

Figure 8. Scheme for the effect of PVP, PNaA, and NaA on CO activity of Au/TiO_2 catalysts

Conclusions

It is exceptionally challenging to determine the specific role of stablisers supported metal catalysts. In this work, we used NaA, PNaA, PVA, and PVP as model ligands to investigate how the ligand effects on Au catalysis. UV-Vis spectra and HPLC analysis indicate that NaA formed strong electronic interaction with $HAuCl_4$ in solution and most of feed NaA remained on the catalysts. When tested in CO oxidation, NaA stabilized catalysts demonstrated the highest activity, followed by PNaA, while PVP and PVA showed negative effect for the catalysis compared to Au/TiO_2 (none) without ligand. When reducing the water in synthesis, Au/TiO_2 (none) showed significant growth in Au NPs and very low activity for CO oxidation, while stabilized catalysts showed only a slight increase from original Au NPs particle size. Once again, Au/TiO_2 (NaA) had a higher activity than catalysts stabilized by PNaA, PVP, and PVA. From the composition analysis, XPS, CO DRIFTS, HRTEM, and XAS characterization, we found the activity increased with the amount of low coordinated step/kink Au sites. The catalysts with NaA with higher activity also tended to contain a higher proportion of small, wetted particles with a higher level of metal-support interfacial sites. From the results presented herein, it is evident that the physicochemical properties of stabilizers, used in the synthesis of supported metal catalysts, can dramatically influence catalytic activity. We have demonstrated that their presence can sterically inhibit reactivity and thus, remain present throughout the

reaction. We therefore consider it of interest to next assess whether this property might influence chemoselectivity in the transformation of more functionalized substrates; an interesting perspective, which requires further exploration.

Supporting information. SEM, XPS, TGA-MS, XRD, TEM, EXAFS characterisation of catalysts and further catalyst testing data.

Acknowledgements

The authors wish to thank Cardiff University for financial support. The authors would like to thank Thomas Davies for supervision and advice regarding microscopy and the EM facility for providing instrumentation. N. Y. wishes to thank the China Scholarship Council (CSC) for her scholarship.

Conflict of interest

The authors declare no conflict of interest.

References

1. Boyen, H. G.; Kastle, G.; Weigl, F.; Koslowski, B.; Dietrich, C.; Ziemann, P.; Spatz, J. P.; Riethmuller, S.; Hartmann, C.; Moller, M.; Schmid, G.; Garnier, M. G.; Oelhafen, P., Oxidation-resistant gold-55 clusters. *Science* **2002,** *297* (5586), 1533-1536.
2. Grass, M. E.; Zhang, Y.; Butcher, D. R.; Park, J. Y.; Li, Y.; Bluhm, H.; Bratlie, K. M.; Zhang, T.; Somorjai, G. A., A reactive oxide overlayer on Rhodium nanoparticles during CO oxidation and its size dependence studied by In situ ambient-pressure X-ray photoelectron spectroscopy. *Angew Chem Int Ed* **2008,** *47* (46), 8893-8896.
3. Jin, M.; Liu, H.; Zhang, H.; Xie, Z.; Liu, J.; Xia, Y., Synthesis of Pd nanocrystals enclosed by {100} facets and with sizes < 10 nm for application in CO oxidation. *Nano Res* **2011,** *4* (1), 83-91.
4. Collins, G.; Davitt, F.; O'Dwyer, C.; Holmes, J. D., Comparing Thermal and Chemical Removal of Nanoparticle Stabilizing Ligands: Effect on Catalytic Activity and Stability. *ACS Appl Nano Mater* **2018,** *1* (12), 7129-7138.
5. Haruta, M.; Yamada, N.; Kobayashi, T.; Iijima, S., Gold catalysts prepared by coprecipitation for low-temperature oxidation of hydrogen and of carbon monoxide. *J Catal* **1989,** *115* (2), 301-309.
6. Haruta, M.; Kobayashi, T.; Sano, H.; Yamada, N., Novel gold catalysts for the oxidation of carbon monoxide at a temperature far below 0 °C. *Chem Lett* **1987,** (2), 405-408.
7. Hutchings, G. J., Vapor phase hydrochlorination of acetylene: Correlation of catalytic activity of supported metal chloride catalysts. *J Catal***1985,** *96* (1), 292-295.
8. Haruta, M., When gold is not noble: catalysis by nanoparticles. *Chem Rec* **2003,** *3* (2), 75-87.
9. Dimitratos, N.; Lopez-Sanchez, J. A.; Hutchings, G. J., Slective liquid phase oxidation with supported metal nanoparticles. *Chem Sci* **2012,** *3* (1), 20-44.
10. Haruta, M., Catalysis of gold nanoparticles deposited on metal oxides. *Cattech* **2002,** *6* (3), 102-115.
11. Hashmi, A. S. K.; Hutchings, G. J., Gold catalysis. *Angew ChemInt Ed* **2006,** *45* (47), 7896-7936.
12. Corma, A.; Garcia, H., Supported gold nanoparticles as catalysts for organic reactions. *Chem Soc Rev* **2008,** *37* (9), 2096-2126.
13. Widmann, D.; Behm, R. J., Activation of Molecular Oxygen and the Nature of the Active Oxygen Species for CO Oxidation on Oxide Supported Au Catalysts. *Acc Chem Res* **2014,** *47* (3), 740-749.
14. Green, I. X.; Tang, W. J.; Neurock, M.; Yates, J. T., Spectroscopic Observation of Dual Catalytic Sites During Oxidation of CO on a Au/TiO_2 Catalyst. *Science* **2011,** *333* (6043), 736-739.
15. Min, B. K.; Friend, C. M., Heterogeneous gold-based catalysis for green chemistry: Low-temperature CO oxidation and propene oxidation. *Chem Rev* **2007,** *107* (6), 2709-2724.
16. Hvolbaek, B.; Janssens, T. V. W.; Clausen, B. S.; Falsig, H.; Christensen, C. H.; Norskov, J. K., Catalytic activity of Au nanoparticles. *Nano Today* **2007,** *2* (4), 14-18.
17. Daté, M.; Haruta, M., Moisture Effect on CO Oxidation over Au/TiO_2 Catalyst. *J Catal* **2001,** *201* (2), 221-224.
18. Saavedra, J.; Doan, H. A.; Pursell, C. J.; Grabow, L. C.; Chandler, B. D., The critical role of water at the gold-titania interface in catalytic CO oxidation. *Science* **2014,** *345* (6204), 1599-1602.
19. Murayama, T.; Haruta, M., Preparation of gold nanoparticles supported on Nb_2O_5 by deposition precipitation and deposition reduction methods and their catalytic activity for CO oxidation. *Chinese J Catal* **2016,** *37* (10), 1694-1701.
20. Villa, A.; Wang, D.; Veith, G. M.; Vindigni, F.; Prati, L., Sol immobilization technique: a delicate

balance between activity, selectivity and stability of gold catalysts. *Catal Sci Technol* **2013,** *3* (11), 3036.
21. Baatz, C.; Decker, N.; Pruesse, U., New innovative gold catalysts prepared by an improved incipient wetness method. *J Catal* **2008,** *258* (1), 165-169.
22. Prati, L.; Villa, A., The Art of Manufacturing Gold Catalysts. *Catalysts* **2012,** *2* (1), 24-37.
23. Campisi, S.; Schiavoni, M.; Chan-Thaw, C.; Villa, A., Untangling the Role of the Capping Agent in Nanocatalysis: Recent Advances and Perspectives. *Catalysts* **2016,** *6* (12), 185.
24. Lopez-Sanchez, J. A.; Dimitratos, N.; Hammond, C.; Brett, G. L.; Kesavan, L.; White, S.; Miedziak, P.; Tiruvalam, R.; Jenkins, R. L.; Carley, A. F.; Knight, D.; Kiely, C. J.; Hutchings, G. J., Facile removal of stabilizer-ligands from supported gold nanoparticles. *Nature Chem* **2011,** *3* (7), 551-556.
25. Zhong, R.-Y.; Sun, K.-Q.; Hong, Y.-C.; Xu, B.-Q., Impacts of Organic Stabilizers on Catalysis of Au Nanoparticles from Colloidal Preparation. *ACS Catal* **2014,** *4* (11), 3982-3993.
26. Li, D.; Wang, C.; Tripkovic, D.; Sun, S.; Markovic, N. M.; Stamenkovic, V. R., Surfactant removal for colloidal nanoparticles from solution synthesis: The effect on catalytic performance. *ACS Catal* **2012,** *2* (7), 1358-1362.
27. Cargnello, M.; Chen, C.; Diroll, B. T.; Doan-Nguyen, V. V.; Gorte, R. J.; Murray, C. B., Efficient removal of organic ligands from supported nanocrystals by fast thermal annealing enables catalytic studies on well-defined active phases. *J Am Chem Soc* **2015,** *137* (21), 6906-11.
28. Ansar, S. M.; Arneer, F. S.; Hu, W.; Zou, S.; Pittman, C. U., Jr.; Zhang, D., Removal of molecular adsorbates on gold nanoparticles using sodium borohydride in water. *Nano Lett* **2013,** *13* (3), 1226-1229.
29. Aliaga, C.; Park, J. Y.; Yamada, Y.; Lee, H. S.; Tsung, C.-K.; Yang, P.; Somorjai, G. A., Sum frequency generation and catalytic reaction studies of the removal of organic capping agents from Pt nanoparticles by UV-Ozone treatment. *J Phys Chem C* **2009,** *113* (15), 6150-6155.
30. Liu, P.; Qin, R.; Fu, G.; Zheng, N., Surface Coordination Chemistry of Metal Nanomaterials. *J Am Chem Soc* **2017,** *139* (6), 2122-2131.
31. Gorin, D. J.; Sherry, B. D.; Toste, F. D., Ligand effects in homogeneous Au catalysis. *Chem Rev* **2008,** *108* (8), 3351-78.
32. Jin, L.; Liu, B.; Duay, S.; He, J., Engineering Surface Ligands of Noble Metal Nanocatalysts in Tuning the Product Selectivity. *Catalysts* **2017,** *7* (12), 44.
33. Tsunoyama, H.; Ichikuni, N.; Sakurai, H.; Tsukuda, T., Effect of electronic structures of Au clusters stabilized by poly(N-vinyl-2-pyrrolidone) on aerobic oxidation catalysis. *J Am Chem Soc* **2009,** *131* (20), 7086-7093.
34. Lari, G. M.; Nowicka, E.; Morgan, D. J.; Kondrat, S. A.; Hutchings, G. J., The use of carbon monoxide as a probe molecule in spectroscopic studies for determination of exposed gold sites on TiO_2. *Phys Chem Chem Phys* **2015,** *17* (35), 23236-44.
35. Qian, H.; Zhu, M.; Wu, Z.; Jin, R., Quantum Sized Gold Nanoclusters with Atomic Precision. *Acc Chem Res* **2012,** *45* (9), 1470-1479.
36. Deraedt, C.; Salmon, L.; Gatard, S.; Ciganda, R.; Hernandez, R.; Ruiz, J.; Astruc, D., Sodium borohydride stabilizes very active gold nanoparticle catalysts. *Chem Commun* **2014,** *50* (91), 14194-14196.
37. Porta, F.; Prati, L.; Rossi, M.; Coluccia, S.; Martra, G., Metal sols as a useful tool for heterogeneous gold catalyst preparation: reinvestigation of a liquid phase oxidation. *Catal Today* **2000,** *61* (1-4), 165-172.
38. Xu, W. W.; Gao, Y.; Zeng, X. C., Unraveling structures of protection ligands on gold nanoparticle Au-68(SH)(32). *Sci Adv* **2015,** *1* (3), e1400211.

39. Wang, H.; Gu, X. K.; Zheng, X.; Pan, H.; Zhu, J.; Chen, S.; Cao, L.; Li, W. X.; Lu, J., Disentangling the size-dependent geometric and electronic effects of palladium nanocatalysts beyond selectivity. *Sci Adv* **2019,** *5* (1), eaat6413.
40. Shang, Y.; Min, C.; Hu, J.; Wang, T.; Liu, H.; Hu, Y., Synthesis of gold nanoparticles by reduction of HAuCl4 under UV irradiation. *Solid State Sci* **2013,** *15*, 17-23.
41. Nemanashi, M.; Meijboom, R., Catalytic Behavior of Different Sizes of Dendrimer-Encapsulated Au-n Nanoparticles in the Oxidative Degradation of Morin with H_2O_2. *Langmuir* **2015,** *31* (33), 9041-9053.
42. Villa, A.; Dimitratos, N.; Chan-Thaw, C. E.; Hammond, C.; Veith, G. M.; Wang, D.; Manzoli, M.; Prati, L.; Hutchings, G. J., Characterisation of gold catalysts. *Chem Soc Rev* **2016,** *45* (18), 4953-94.
43. Xiong, Y. J.; Washio, I.; Chen, J. Y.; Cai, H. G.; Li, Z. Y.; Xia, Y. N., Poly(vinyl pyrrolidone): A dual functional reductant and stabilizer for the facile synthesis of noble metal nanoplates in aqueous solutions. *Langmuir* **2006,** *22* (20), 8563-8570.
44. Deraedt, C.; Salmon, L.; Gatard, S.; Ciganda, R.; Hernandez, R.; Ruiz, J.; Astruc, D., Sodium borohydride stabilizes very active gold nanoparticle catalysts. *Chem Commun* **2014,** *50* (91), 14194-6.
45. Comotti, M.; Li, W. C.; Spliethoff, B.; Schuth, F., Support effect in high activity gold catalysts for CO oxidation. *J Am Chem Soc* **2006,** *128* (3), 917-924.
46. Raphulu, M.; McPherson, J.; Pattrick, G.; Ntho, T.; Mokoena, L.; Moma, J.; van der Lingen, E., CO oxidation: Deactivation of Au/TiO_2 catalysts during storage. *Gold Bull* **2009,** *42* (4), 328-336.
47. Grunwaldt, J. D.; Maciejewski, M.; Becker, O. S.; Fabrizioli, P.; Baiker, A., Comparative study of Au/TiO_2 and Au/ZrO_2 catalysts for low-temperature CO oxidation. *J Catal* **1999,** *186* (2), 458-469.
48. Mihaylov, M.; Gates, B. C.; Fierro-Gonzalez, J. C.; Hadjiivanov, K.; Knoezinger, H., Redox behavior of gold species in zeolite NaY: Characterization by infrared spectroscopy of adsorbed CO. *J Phys Chem C* **2007,** *111* (6), 2548-2556.
49. Hvolbæk, B.; Janssens, T. V. W.; Clausen, B. S.; Falsig, H.; Christensen, C. H.; Nørskov, J. K., Catalytic activity of Au nanoparticles. *Nano Today* **2007,** *2* (4), 14-18.
50. Dimitratos, N.; Villa, A.; Prati, L.; Hammond, C.; Chan-Thaw, C. E.; Cookson, J.; Bishop, P. T., Effect of the preparation method of supported Au nanoparticles in the liquid phase oxidation of glycerol. *Appl Catal A-Gen* **2016,** *514*, 267-275.
51. Schubert, M. M.; Hackenberg, S.; van Veen, A. C.; Muhler, M.; Plzak, V.; Behm, R. J., CO oxidation over supported gold catalysts-"inert" and "active" support materials and their role for the oxygen supply during reaction. *J Catal* **2001,** *197* (1), 113-122.